Title: DHPAC, a novel synthetic microtubule destabilizing agent, possess high anti-tumor activity in vincristine-resistant oral epidermoid carcinoma *in vitro* and *in vivo*

Authors: Ying Zhang, Fu-Lian Gong, Zhen-Ning Lu, Hong-Yuan Wang, Yan-Na Cheng, Zhao-Peng Liu, Lu-Gang Yu, Hui-Hui Zhang, Xiu-Li Guo

PII: S1357-2725(17)30270-4
DOI: https://doi.org/10.1016/j.biocel.2017.10.012
Reference: BC 5241

To appear in: *The International Journal of Biochemistry & Cell Biology*

Received date: 8-6-2017
Revised date: 15-10-2017
Accepted date: 21-10-2017

Please cite this article as: Zhang, Ying., Gong, Fu-Lian., Lu, Zhen-Ning., Wang, Hong-Yuan., Cheng, Yan-Na., Liu, Zhao-Peng., Yu, Lu-Gang., Zhang, Hui-Hui., & Guo, Xiu-Li., DHPAC, a novel synthetic microtubule destabilizing agent, possess high anti-tumor activity in vincristine-resistant oral epidermoid carcinoma in vitro and in vivo.*International Journal of Biochemistry and Cell Biology* https://doi.org/10.1016/j.biocel.2017.10.012

DHPAC, a novel synthetic microtubule destabilizing agent, possess high anti-tumor activity in vincristine-resistant oral epidermoid carcinoma *in vitro* and *in vivo*

Ying Zhang[1], Fu-Lian Gong[1], Zhen-Ning Lu[1], Hong-Yuan Wang[1], Yan-Na Cheng[1], Zhao-Peng Liu[2], Lu-GangYu[3], Hui-Hui Zhang[1], Xiu-Li Guo*[1]

[1]Department of Pharmacology, Key Laboratory of Chemical Biology (Ministry of Education), School of Pharmaceutical Sciences, Shandong University, Jinan, 250012, P. R. China;

[2]Department of Medicinal Chemistry, School of Pharmaceutical Sciences, Shandong University, Jinan, 250012, P. R. China;

[3]Department of Gastroenterology, Institute of Translational Medicine, University of Liverpool, Liverpool, L69 3GE, UK.

*Correspondence should be addressed to

Xiu-Li Guo

No. 44 Wen Hua Xi Road, Department of Pharmacology, School of Pharmaceutical Sciences, Shandong University, Jinan 250012, P.R. China

Fax: +86-531-88382490

Telephone: +86-531-88382490

E-mail: guoxl@sdu.edu.cn

Graphical abstract

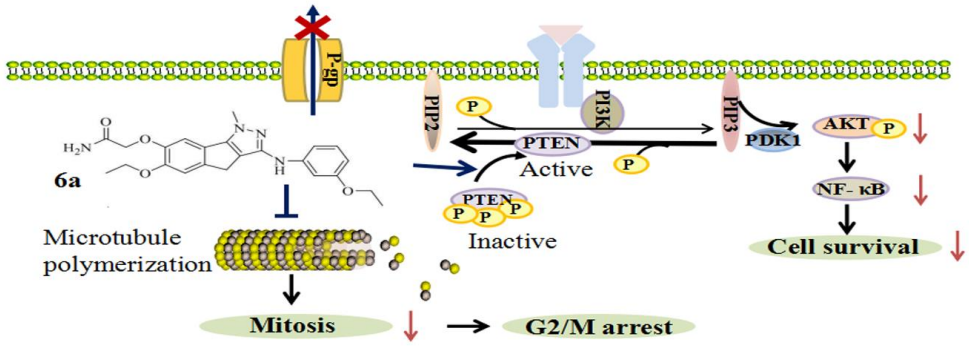

DHPAC, a novel synthetic microtubule destabilizing agent, possess high anti-tumor activity in vincristine-resistant oral epidermoid carcinoma *in vitro* and *in vivo*

Abstract

Multidrug resistance (MDR) is one of major obstacles to effective chemotherapeutic treatment of cancer. This study showed that DHPAC, 2-(6-ethoxy-3-(3-ethoxyphenylamino) -1-methyl-1,4-dihydroindeno[1,2-c]pyrazol-7-yloxy) acetamide, a novel compound that binds to the same site on microtubules as colchicine, has high anti-tumour activity in vincristine-resistant oral epidermoid carcinoma (KB/V) cells. It found that the presence of DHPAC strongly inhibited KB/V cell growth *in vivo* and in mice xenograft. The inhibitory effect of DHPAC is much stronger than that by colchicine in these KB/V cells (IC_{50}: 64.4 nM and 458.0nM respectively). Treatment of the cells with DHPAC induced cell apoptosis by reducing mitochondrial membrane potential and altered the expression of several apoptosis-related proteins such as Bcl-2, Bax, Caspase-9, Cytochrome c and PARP. DHPAC treatment also caused cell rest in G2/M phase by regulating of the expression of a number of cell cycle-related proteins (e.g. Cyclin B1, Cdc2, Cdc25b, Cdc25c, RSK2). Furthermore,

DHPAC presence inhibits PTEN phosphorylation and PTEN/Akt/NF-κB signalling. Thus, DHPAC has potent anti-cancer activity in MDR tumuors and may be a potential therapeutic agent for the treatment of vincristine-resistant human oral epidermoid carcinoma.

Key Words:

Multidrug-resistance

KB/V cells

Microtubule destabilizing agent

Colchicine binding site

PTEN/Akt/NF-κB signal pathway

1. Introduction

Multidrug resistance (MDR), in which tumor cells develop cross-resistance to classes of functionally and structurally unrelated antitumor drugs (Abdallah et al., 2015), is one of the most common problems in the treatment of malignant tumors. Overexpression of drug efflux proteins such as P-glycoprotein (P-gp), alteration of topoisomerase II activities, and mutation of P53 by tumor cells are all believed to contribute to MDR in cancer treatment (Luqmani, 2005). P-gp (ABCB1) is a 170-kDa transmembrane protein and a member of ATP-binding cassette (ABC) transporters. It is intrinsically over-expressed in many types of tumors such as colon, rectum, liver, and kidneys (Patel and Rothenberg, 1994). Research approaches try to overcome P-gp-associated drug resistance include that the use of anti-cancer drugs with novel P-gp inhibitors (Binkhathlan and Lavasanifar, 2013).

Microtubules are key components of the cytoskeleton with polymerizing α-tubulin and

β-tubulin heterodimers. They play important roles in maintaining cell shape, proliferation, division, signaling, and trafficking in eukaryotic cells (Perez, 2009; Jordan and Wilson, 2004). Because of its ability of forming mitotic spindle that affects segregation of the replicated chromosome during cell division, microtubules are excellent drug targets for tumor therapy (Parker et al., 2014). Some tubulin binding agents (e.g. vinca alkaloids, colchicine) have shown to inhibit microtubule polymerization and some others (such as taxanes), have shown to inhibit microtubule depolymerization (Yan et al., 2015).

The microtubule binding agent colchicine was approved by FDA in 2009 as a mono-therapy drug to treat familial mediterranean fever and acute gout flares (Lu et al., 2012), but is no longer used as a chemotherapeutic drug in clinic due to its high cytotoxicity. Diverse efforts have been made over the past years to develop new agents that can target the same colchicine binding site on microtubules to prevent neovascularization and multidrug resistance (MDR) (Lu et al., 2012). DHPAC, 2-(6-ethoxy-3-(3-ethoxyphenylamino)-1-methyl-1,4-dihydroindeno[1,2-c] pyrazol-7-yloxy) acetamide, is a novel synthetic compound that has high binding affinity toward the same colchicine binding site on microtubules and exhibits potent anti-tumor activity on non-small cell lung cancer (NSCLC) (Liu et al., 2016). This study investigated the anti-tumor effect of DHPAC *in vitro* and *in vivo* of vincristine-resistant oral epidermoid carcinoma cells (KB/V cells) with P-gp overexpression. It found that the anti-tumour activity of DHPAC is closely related to its inhibition of tubulin polymerization and PTEN/Akt/NF-κB signalling.

2. Materials and Methods

2.1 Compounds

Compound DHPAC and colchicine (Figure 1) were synthesized at Institute of Medicinal Chemistry, School of Pharmaceutical Sciences, Shandong University. Compound DHPAC, white solid, mp 186−188°C; ^{1}H NMR (600 MHz, DMSO-d_6) δ 1.32 (t, J = 7.2 Hz, 3H), 1.37 (t, J = 7.2 Hz, 3H), 3.39 (s, 2H), 3.94 (s, 3H), 3.98 (q, J = 7.2 Hz, 2H), 4.10 (q, J = 7.2 Hz, 2H), 4.53 (s, 2H), 6.30 (dd, J = 8.4,1.8 Hz, 1H), 6.83 (dd, J = 8.4,1.8 Hz, 1H), 6.98(t, J = 1.8 Hz, 1H), 7.06 (t, J = 7.8 Hz, 1H), 7.27 (s, 1H), 7.37 (s, 1H), 7.39 (s, 1H), 7.50 (s, 1H), 8.38 (s, 1H); ^{13}C NMR (100 MHz, DMSOd_6) δ 170.9, 159.7, 148.6, 147.9, 147.2, 145.4, 144.9, 143.4, 129.8, 124.9, 112.8, 112.7, 108.3, 107.6, 104.4, 101.9, 69.8, 64.7, 63.1, 37.5, 29.5, 15.3; MS (ESI) m/z 423.4 $(M + H)^+$, 445.5 $(M + Na)^+$; Anal. calcd for $C_{23}H_{26}N_4O_4$ (Liu et al., 2016). DHPAC and colchicine were both dissolved in dimethyl sulfoxide (DMSO) and stored at -20°C.

2.2 Materials

Paclitaxel was obtained from Sangon Biotech (Shanghai, China) with purity > 98%. Vincristine sulfate was purchased from Lingnan Pharmaceutical LTD (Guangzhou, China). Doxorubicin freeze drying agent was purchased from Pfizer (Actavis, Italy). Fluorouracil Injection was purchased from Shanghai XudongHaipu Pharmaceutical CO. LDT (Shanghai, China). Verapamil Hydrochloride Injection was obtained from Shanghai Harvest Pharmaceuticals (Shanghai, China). Trypsin solution, crystal violet dye,3-(4, 5-dimethylthiazol-2-yl)-2, 5-diphenyl tetrazolium bromide (MTT), propidium iodide (PI), bovine serum albumin (BSA), hoechst 33342 and phenylmethanesulfonyl fluoride (PMSF) were purchased from Solarbio technology (Beijing, China). Radio immunoprecipitation assay (RIPA) lysis buffer, JC-1 fluorescence probekit, rhodamine123 (Rh123) were purchased from

Beyotime biotechnology (Shanghai, China). Annexin V-FITC apoptosis detection Kit was purchased from 4A Biotech. (Beijing, China). Z-VAD-FMK was purchased from Selleck (Shanghai,China). Monoclonal antibodies against Bax, Bcl-2, caspase 9, caspase 3, PARP, Phospho-cdc2 (p-cdc2, Tyr15), cdc2, cyclin B1, cdc25B, Phospho-Akt (p-Akt, Ser473), PI3K, Phospho-PTEN (p-PTEN, Ser380/Thr382/Thr383), NF-κB, P-glycoprotein (P-gp) and α-tubulin were purchased from Cell Signaling Technology (CST, Boston, MA, USA). Monoclonal antibodies against PTEN, cytochrome c, caspase 8, RSK2 and Akt were purchased from proteintech (Wuhan, China), RPMI-1640 medium, fetal bovine serum was purchased from Gibco (Gaithersburg, MD, USA).

2.3 Cell Culture

Human oral epidermoid carcinoma cell line KB, human breast cancer cell line MCF-7, Adriamycin (ADR) selected MDR subline MCF-7/ADR and human hepatocellular carcinoma cell line BEL7402, 5-fluorouracil (5-FU) selected MDR subline BEL7402/5-FU were purchased from American Type Culture Collection (ATCC, Manassas, VA, USA). Vincristine (VCR) selected MDR subline KB/V was obtained from Sun Yat-Sen University of Medical Sciences (Guangzhou, China). All of these cells were cultured in RPMI-1640 medium supplemented with 10% FBS at 37°C in a humidified atmosphere of 5% CO_2 and 95% air. In order to maintain the MDR phenotype, KB/V cells were cultured in medium with 40 nM vincristine, K562/A02 cell with 1μM doxorubicin and BEL7402/5-FU with 2 mM 5-fluorouracil. Drugs were removed one week before the experiment (Xu et al., 2012; Yang et at., 2012; Yue et al., 2013).

2.4 Cell proliferation assay

The inhibitory effects of different compounds on the proliferation of various human cancer cell lines and multidrug resistant cell lines were measured by the MTT assay. Briefly, cells (800~2000 per well) were seeded into 96-well plates and grown for 24 h before treatment with various concentrations of compounds for a further 24 h or 48h. 20 μL of MTT solution (5mg /mL) was added to each well for 4h at 37 °C. Then the formazan crystals were dissolved in 200 μL of DMSO solution before the absorbance was measured using the Thermo Multiskan GO microplate reader (Thermo-1510, CA, USA) at a wavelength of 570 nm (Zhao et al., 2012).

2.5 Colony formation assay

KB/V cells (300 per well) seeded into 6-well plates were treated with different concentrations (20, 30, 40 nM) of DHPAC for 24h, and then were cultured in drug-free medium for 10 days. Colonies were fixed in ice-cold methanol/glacial acetic acid (3:1, v/v) for 10 minutes and stained with 0.8% crystal violet, and then were imaged and counted under the microscope (CKX31SF, Olympus, Japan).

2.6 Rhodamine 123 (Rh123) accumulation assay

KB/V cells (3.5×10^5 per well) seeded into 24-well plates were treated with different concentrations (20, 40, 80 nM) of DHPAC or 10.0 μM verapamil (Ver) (positive control) for 3h. KB cells were treated with vehicle as negative control. Then 5μM Rh123 was added to each well in dark at 37°C for 1h. After washing cells with ice-cold phosphate buffered saline (PBS) repeatedly, the images were taken by fluorescence microscopy (200×, TE2000-S; Nikon, Tokyo, Japan).

2.7 Immunofluorescence staining

KB/V cells were seeded into 24-well plate (with coverslips inserted) at density of 4×10^4 cells per well. After overnight culture at 37℃, cells were exposed to DHPAC (20 or 80nM) or colchicine (80nM) for 24 h. The cells were fixed with ice-cold methanol/glacial acetic acid (3:1) for 10 min and blocked with 3% bovine serum albumin (BSA) in PBS for 20 min at room temperature. Then cells were incubated with a mouse anti-α-tubulin antibody (1:200) overnight at 4°C and followed by reaction with FITC-conjugated secondary antibody (1:500) for 2h at 37℃. Finally, cells were stained with hoechst 33342 to mark the nuclear, and fluorescence images were taken with fluorescence microscope (200×, TE2000-S; Nikon, Tokyo, Japan).

2.8 Nuclear morphology analysis

KB/V cells were seeded in 24-well plates at a density of 4×10^4 cells per well. After introduction of various concentrations of DHPAC for 24 h, the cells were fixed in 4% paraformaldehyde in PBS for 30min, and then stained with hoechst 33324 (10μg/ml) in dark at room temperature for 15 min. After three washes with PBS, the cells were visualized with fluorescence microscopy (200×, TE2000-S; Nikon, Tokyo, Japan).

2.9 Annexin V/PI staining assay

KB/V cells seeded in 6-well plate (2×10^5 per well) were treated with DHPAC (20nM, 40nM, 80nM) or colchicine (80nM) for 48h. The cells were harvested, washed with cold PBS and the cell surface phosphatidylserine in apoptotic cells was determined using AnnexinV/FITC and PI apoptosis detectionkit (ydjmbio, China) according to manufacturer's instructions and analyzed by a FACScan flowcytometry (Becton Dickinson, Franklin Lakes, New Jersey, USA) using emission filters of 525 and 575 nm respectively (Lu et al., 2015;

Wang et al., 2016).

2.10 Cell cycle analysis

KB/V cells (5×10^5 cells per well) were plated in 60mm plates and exposed to 20nM, 40nM, 80nM DHPAC or 80nM colchicine for 24 h. The cells were harvested, washed twice with cold PBS and fixed with pre-cooled 70% ethanol at -20°C overnight. After washing with PBS twice, the cells were incubated with RNase A (100 μg/mL) for 30 min at 37 °C before addition of propidium iodide (PI) for DNA staining in the dark at 4°C for 15 min. Cell cycle distribution was analyzed and quantified using a FACSort flow cytometry (Beckman coulter, USA).

2.11 Western Blotting analysis

After treatment with DHPAC, cells were harvested and lysed with lysis buffer containing proteinase inhibitors (PMSF) at 99:1, v/v. With centrifuging at 15000g for 15 min, the total protein concentrations were determined using BCA protein assay kit (Thermo Scientific, USA). Loading buffer (Beyotime, China) was added into each samples and the samples were heated at 100°C for 5 min. Cell lysates were subjected to 10% SDS-polyacrylamide gel electrophoresis (PAGE) followed by protein transfer to a PVDF membranes (Millipore, USA) and probed with primary antibodies (1:1000) against P-gp, cyclin B1, p-cdc2, cdc2, cdc25B, cdc25C, RSK2, PARP, caspase 9, caspase 3, caspase 8, Bcl-2, Bax, cytochrome c, PTEN, p-PTEN, p-Akt, Akt, PI3K, NF-κB and β-actin (1:1000 in primary antibody diluent) at 4°C overnight. Immunoblots were developed using horseradish peroxidase (HRP)-conjugated secondary antibodies (1:10000), and visualized by the enchanced chemiluminescent (ECL) system (Millipore, Billerica, MD, USA) and quantified by densitometry using a ChemiDoc

XRS (Bio-Rad, Hercules, California, USA). There relative intensity of each band was normalized to β-actin.

2.12 Measurement of mitochondrial membrane potential

Mitochondrial membrane potential (MMP) was evaluated by using fluorescent carbocyanine dye JC-1 which can selectively enter mitochondria and reversibly change color from red to green as the MMP decreased (Otera and Mihara, 2012). KB/V cells (1.5×10^5 cells per well) seeded in 6-well plates were exposed to 20nM, 40nM, 80nM DHPAC or 80nM colchicine for 48h. Cells were harvested and incubated with JC-1 for 20 min at 37 °C. Fluorescence intensity was measured immediately by FACSort flow cytometer (Beckman coulter, USA).

2.13 Assessment of DHPAC antitumor activity *in vivo*

Five-week-old female Balb/C nude mice were purchased from the Animal Centre of China Academy of Medical Sciences (Beijing, China) and acclimated and caged in 5 groups. Animals were housed under pathogen-free conditions. The research protocol was in accordance with the Institutional Guidelines of Animal Care and Use Committee of Shandong University. After one week of feeding, KB/V xenografts were established by inoculating 8.0×10^6 KB/V cells subcutaneously into armpit of nude mice under sterile conditions. When the xenografts volume reached approximately 500 mm^3, the animals were sacrificed and the tumors were extracted and cut into 1 mm^3 fragments (about 20mg/fragment). One fragment was transplanted subcutaneously into the right flank by trocar in each nude mouse. When the solid tumor reached a volume of 100 mm^3 to 200 mm^3, the mice were divided into six groups (n=6) at random: blank control group (normal saline), vehicle control group (Castor Oil:

ethanol: dextrose 5% in water (D5W) = 1:1:4), DHPAC (15 mg/kg, 30 mg/kg) group, and paclitaxel (10mg/kg) group. DHPAC and vehicle were given every day by intraperitoneal injection for 20 days. Paclitaxel was given 7 days then suspended for 3 days, followed by 10 days injection. The tumor and body weight of the mice were measured every 3 days. Tumor volume was calculated as $W^2 \times L/2$. At the end of the experiment, the mice were sacrificed and the xenografts were removed and weighed. Effect of DHPAC on tumor growth was expressed as a percentage to that in the vehicle control group.

2.14 Statistical analysis

All quantitative dates are expressed as mean ± SD. Statistical comparisons were performed by one-way analysis of variance. A P-value < 0.05 was considered statistically significant. Statistical analysis was performed using the SPSS/Win 13.0 software.

3. Results

3.1 DHPAC inhibits KB/V cells proliferation *in vitro*

The phenotype of MDR in KB/V, Bel7402/5-FU, and MCF-7/ADR cells was determined by MTT assay. In comparison with their parental cells, MDR cells showed significant resistance to cytotoxic killing by VCR, 5-FU or ADR, respectively. As shown in Table 1, a > 164-fold increase of resistance for 5-FU in Bel7402/5-FU cells, a > 115-fold increase of resistance for VCR and a > 29 increase for paclitaxel in KB/V cells were observed. The anti-proliferative activity of DHPAC or colchicine against the above MDR cancer cells and their parental cells were also determined by MTT assay (Table 2). All the three MDR cell lines exhibited resistance to colchicine. DHPAC showed to induce similar inhibitory effects

on the growth of MCF-7/ADR and Bel7402/5-FU cells as colchicine, but better inhibition than colchicine, vincristine or paclitaxel on the growth of KB/V cells (IC_{50} value was 64.4 nM for DHPAC, 458.0 nM for colchicine, 427.3 nM for vincristine, 574.9 nM for paclitaxel). These indicated an excellent anti-proliferative activity of DHPAC in KB/V cells. Moreover, DHPAC at concentrations from 6.25 nM to 100 nM inhibited the proliferation of KB/V and KB cells in a dose-dependent manner, while the IC_{50} values of colchicine in KB/V cells were much bigger than that in KB cells at different time points (IC_{50} value were 458.0, 138.2, 120.0 nM in KB/V and 33.1, 14.6, 7.6 nM in KB cells). (Table 3 and Figure 2B).

The cytotoxicity of DHPAC in KB/V cells was further evaluated by colony formation assay. As shown in Figure 2A, the presence of DHPAC at the concentrations 20 nM to 40 nM showed 30.3%, 67.7%, 93.1%, respectively, inhibition of colony formation of KB/V cells. Colchicine at 40 nM showed to cause 17.2% inhibition of colony formation of these cells. At equal dosage (e.g.40nM) DHPAC also showed stronger inhibition of colony formation than colchicine ($p < 0.01$).

3.2 DHPAC inhibits tumor growth in mice implanted with KB/V cells

Administration of DHPAC resulted in significant inhibition on growth of KB/V tumor xenografts in nude mice (Figure 2C, Table 4). Treatment of nude mice with DHPAC at 30mg/kg by intraperitoneal injection resulted in 75.8 % reduction of tumor growth ($p < 0.01$) after 20 days in comparison to the vehicle control group (Castor Oil: ethanol: dextrose 5% in water (D5W) = 1:1:4). Administration of paclitaxel at 10mg/kg caused 24.1% growth inhibition. There were no significant difference of tumour size and body weight between the vehicle control and blank control groups, indicating no inhibitory and cytoxic activity of the

vehicle. The animals demonstrated general tolerance with DHPAC treatment and weak loss of the body weight was observed only in high dose group. On the other hand, the animals administrated with paclitaxel showed dramatic reduction of body weight from day 6 (Figure. 2D).

3.3 DHPAC is not a substrate of P-gp efflux pump and has no effect on the activity and expression of P-gp in KB/V cells

Rhodamine-123 (Rh123) is a low toxic fluorescent probe and is often used to detect the activity of P-gp efflux pump. As illustrated in Figure 3A, the fluorescence intensity (FI) of Rh123 in KB/V cells was much lower than that in KB cells, suggesting higher P-gp activity in KB/V cells. After treatment with 10 μM of verapamil (Ver, inhibitor of P-gp in MDR), the FI in KB/V cells increased significantly in comparison to vehicle-treated KB/V cells. No significant difference of the FI was seen in KB/V cells treated with either different concentrations of DHPAC or colchicine in comparison with vehicle-treated KB/V cells. P-gp expression was much higher in KB/V cells than in KB cells when analyzed by Western blot. The presence of DHPAC at 20, 40, 80 nM or colchicine at 80 nM had no obvious effects on P-gp expression in KB/V cells (Figure 3B).

3.4 DHPAC inhibits tubulin polymerization and induces G2/M phase arrest in KB/V cells.

The effects of DHPAC on microtubule organization were investigated with immunofluorescence staining of α-tubulin. As shown in Figure 4, the microtubule networks exhibited a normal arrangement with slim and fibrous microtubules wrapped around the cell nucleus in untreated or vehicle-treated cells. However, after the cells treated with DHPAC at 20nM or 80nM for 24h, the microtubule bundles became shorter and disoriented with diffused

fluorescent staining throughout the cytoplasm. Nuclear fragmentation and microtubule condensation were also clearly observed in DHPAC-treated cells. At equal dose of 80 nM, DHPAC again showed better effects than colchicine on inhibition of tubulin polymerization.

It is known that microtubule-targeting agents often regulate the cell cycle by blocking mitosis. Treatment of the cells with DHPAC induced an accumulation of cells in the G2/M phase dose-dependently, whereas the control cells were mainly in the G1 phase. As shown in Figure 5, DHPAC, approximately 90.3% of KB/V cells were arrested at G2/M phase after treatment with 80nM DHPAC for 24h. At similar concentration, colchicine induced 25.5% rest of the cells in the G2/M phase. When association between DHPAC-induced the arrest of G2/M phase and alterations in proteins that regulated cell division were analysed (Figure 5B), DHPAC induced down-regulation of cdc2, p-cdc2 and cdc25B, cdc25C, RSK2, up-regulation of cyclinB1 in a concentration-dependent manner. At 80nM, DHPAC induced stronger down-regulation of cdc2, p-cdc2, cdc25C, RSK2 and cdc25B than colchicine ($P < 0.05$).

3.5 DHPAC induces apoptosis in KB/V cells through regulating the expressions of apoptotic-related proteins and decreasing mitochondrial transmembrane potential

The effects of DHPAC on KB/V cells apoptosis were firstly examined through hoechst 33342 nuclear staining assay. As shown in Figure 6A, treatment of KB/V cells with DHPAC at 40 or 80 nM for 24h increased the number of cells with condensed chromatin (white arrows) and fragmented nuclei (yellow arrows), characteristics of apoptosis, in comparison to vehicle (DMSO)-treated and 80 nM colchicine-treated groups. Apoptosis induction of the cells by DHPAC was confirmed by flow cytometric analysis using PI and Annexin-V-FITC double staining. The cells can be differentiated to normal live cells (Annexin V^-/PI^- cells), early

apoptotic cells (Annexin V^+/PI^- cells), necrosis/late apoptotic cells (Annexin V^+/PI^+ cells) in this analysis. In Figure 6B, at concentrations of 20, 40 and 80 nM for 48h, DHPAC induced 8.5%, 20.9%, and 30.9%, respectively, while colchicine induced only 5.8% apoptosis at 80 nM.

KB/V cells were pretreated with the pan caspase inhibitor Z-VAD (30 μM) for 1 h before exposure to DHPAC. The apoptosis of KB/V cells was determined by Annexin V/PI staining assay using FACScan flow cytometry. Results showed that in the presence of 30 μM z-VAD, the apoptosis rate induced by 80 nM DHPAC had significantly decreased from 23.6% to 12.3%, and the increased cleaved PARP expression induced by DHPAC was also inhibited ($P < 0.05$) in Figure 7.

Mitochondria-mediated apoptosis is controlled by the Bcl-2 family of proteins, with the activation of caspase 9, the decrease in mitochondrial transmembrane potential (MMP) and the cytochrome c releasing. Fluorescent carbocyanine dye JC-1 was used to assess the effect of DHPAC on MMP. As shown in Figure 8A, the red fluorescence of JC-1 (high $\Delta\psi m$) was gradually decreased and the green fluorescence (low $\Delta\psi m$) was correspondingly increased after the treatment of DHPAC or colchicine. At 20, 40, 80 nM of DHPAC, the high $\Delta\psi m$ was decreased by 16.1%, 21.6%, and 46.2%, respectively, while colchicine decreased $\Delta\psi m$ by 14.9%. The pro-apoptotic proteins Bax were seen to be increased and the anti-apoptotic proteins Bcl-2 were decreased after DHPAC treatment. DHPAC at 80nM decreased the ratio of Bcl-2/Bax by 59.2% compared with vehicle control. Meanwhile, the expression of cleaved PARP, cleaved caspase 9 and cytochrome c was increased 10.3, 2.1 and 2.02 times, respectively, in response to 80 nM DHPAC treatment (Figure 8B). However, DHPAC had no

significant effect on the expression of caspase 8.

3.6 DHPAC disrupted PTEN/Akt/NF-κB signal pathway *in vitro* and *in vivo*

PI3K/Akt signal pathway plays a major role in cell survival and is activated in many tumor cells. As shown in Figure 9A, DHPAC treatment of the cells strongly reduced the levels of NF-κB, p-Akt, Akt and p-PTEN in a dose-dependent manner in KB/V cells. It also induced a weak decrease on the expression of PI3K, while had no significant effect on PTEN expression. Moreover, cytoplasmic as well as nuclear localization of NF-κB, was markedly decreased by the treatment of DHPAC (Figure 9B). In Figure 9C, after treatment of the cells with bpV (phen), a PTEN inhibitor, DHPAC induced remarkably higher expression of p-Akt and NF-κB in comparison with DHPAC treatment alone. What's more, the expression of p-Akt and NF-κB in co-treatment group of Bpv and DHPAC was lower obviously than Bpv treatment alone. Meanwhile, DHPAC treatment in mouse xenografts of KB/V cells also showed to dramatically decrease the expression of p-PTEN, p-Akt, NF-κB (Figure 9D).

4. Discussion

Computer-aided drug design (CADD) has been increasingly used in drug development, according to provide some useful directions in the optimal design and discovery of anti-cancer drugs. DHPAC is a novel agent which targeted on colchicine binding site at the interface between the α- and β-subunit of tubulin heterodimers in zone 1 and was initially obtained by CADD (Liu et al., 2016). In comparison to the other tubulin binding region (taxane or vinca alkaloid binding sites), targeting the colchicine binding site may provide a better opportunity for structural optimization to overcome drug resistance while complied with Lipinski's Rule

of Five (Hwang et al., 2015; Lipinski et al., 2001). In the present study, the anti-proliferative activity of DHPAC and colchicine (a positive control in vitro assay) against several human MDR cancer cell lines (KB/V cells, MCF-7/A cells, BEL7402/5-FU cells) and their parental cell lines were compared. Results showed that DHPAC has higher anti-tumor selectivity in KB/V cells than colchicine in vitro and in KB/VCR xenografts in nude mice. In the process of mitosis, microtubules undergo rapid polymerization and depolymerization to ensure the movement of chromosomes, essential for cell replication and proliferation. Disruption of microtubule dynamics or reduction of microtubule polymer mass leads to G2/M arrest (Chang et al., 2015). Cdc2 (also called cyclin-dependent kinase 1 (CDK1) and cyclinB1 are the key regulatory proteins of G2/M. Before mitosis, cdc2/cyclinB1 complex accumulates in cytoplasm as an inactive form as a result of cdc2 phosphorylation at Thr14 and Tyr15 (Sur and Agrawal, 2016). Removal of the cdc2 phosphate groups at Thr14/Tyr15 by cdc25 activates the cdc2/cyclinB1 complex and promotes G2 to M transition (Sur and Agrawal, 2016; Bulavin et al., 2003). The activated CDK1/cyclinB1 complex has a positive feedback loop to further activate cdc25. RSK, a 90-kDa ribosomal S6 kinase, plays an important role in the phosphorylation and activation of cdc25 in the process of G2/M transition. RSK2 is the major isoform of RSK which reveals the capacity to activate cdc25C (Wu et al., 2014). Mitosis is blocked in the absence of CDC25 or cdc2/cyclinB1 complex (Deibler and Kirschner, 2010; Loffler et al., 2006). In our study, DHPAC at 80 nM showed to induce disintegration of microtubule skeleton and extensive loss of microtubule mass, characteristics of microtubule depolymerization, an effect that is accompanied by G2/M arrest of the cells. DHPAC also showed better ability to induce microtubule depolymerization and G2/M arrest

than colchicine at the same concentration. DHPAC treatment reduces the expression of cdc2, p-cdc2 (Tyr15), cdc25C, RSK2 and cdc25B, depresses the formation and activation of cdc2/cyclinB1 complex, leading to G2/M arrest.

Many anti-tumor drugs induce G2/M arrest and cell apoptosis (Schwartz and Shah, 2005). Apoptosis is a programmed cell death with two signaling pathways, the extrinsic pathway (the death receptor pathway) and the intrinsic pathway (mitochondrial pathway). Mitochondrial mediated pathway is mainly regulated by Bcl-2 family. In response to apoptotic signals, reduction of the ratio of Bcl-2/Bax decrease the mitochondrial membrane potential (MMP) and causes the release of cytochrome c. The released cytochrome c in cytoplasm activates caspase 9, caspase 3, followed by cleavage of specific substrate proteins, such as PARP (Zhao et al., 2016; Sun et al., 2010). In the present study, DHPAC treatment was observed to induce apoptosis by decreasing the level of MMP and Bcl-2/Bax complex ratio. This resulted in the release of cytochrome c and activation of caspase 9 and PARP cleavage. Combined use of caspase inhibitor V-ZAD with DHPAC leaded to the reduction of apoptosis rate, indicating that DHPAC induced apoptosis was associated with caspase pathway ulteriorly. Moreover, we found that DHPAC had no significant effect on the expression of caspase 8, suggesting that DHPAC induced apoptosis of KB/V cells by intrinsic apoptosis pathway preferentially.

As a regulator of cell survival, PI3K/Akt/NF-κB signaling is constitutively activated in oral carcinogenesis (Watanabe et al., 2009; Amornphimoltham et al., 2004). Dysregulation of PTEN/PI3K/Akt signaling contributes to the development of chemotherapeutic resistance of tumor cells (Hafsi et al., 2012). Phosphatase and tensin homolog deleted on chromosome 10 (PTEN) is a well-known tumor suppressor protein that regulates many cellular processes,

including cell death and proliferation, through the PI3K/Akt/NF-κB signalling (Squarize et al., 2013; Molinolo et al., 2009; Xie et al., 2016). PTEN is composed of five functional domains: a phosphatase domain, a C2 domain, a phosphatidylinositol-4, 5-bisphosphate (PIP2)-binding domain (PBD), a C-terminal tail containing PEST and a PDZ interaction motif for protein-protein interactions (Chalhoub and Baker, 2009). It has been suggested that cytosolic PTEN exists as an inactive conformation with phosphorylation of its C-terminal tail (Vazquez and Devreotes, 2006). Dephosphorylation of p-PTEN resulted in sensitization of the PTEN protein (Fragoso and Barata, 2014; Kohnoh et al., 2016). As a lipid phosphatase to phosphatidylinositol 3,4,5-trisphosphate (PIP3), PTEN mediates transformation of PIP3 to PIP2, while PI3K has the inverse function to transform PIP2 to PIP3 (Wang et al., 2016). In this study, treatment of KB/V cells with DHPAC strongly inhibited phosphorylation of PTEN and Akt, and the expression of Akt and NF-κB (in cytoplasm and nucleus) both *in vitro* and *in vivo*. However, DHPAC had no effect on PTEN expression. To further explore the effect of DHPAC on PTEN/Akt/NF-κB signalling pathway, Bpv (phen), a potent protein phosphotyrosine phosphatase (PTP) inhibitor (Spinelli et al., 2015; Schmid et al., 2004) that inhibits the dephosphorylation of PIP3 by PTEN, was used. Higher expression of p-Akt and NF-κB in co-treatment of DHPAC and Bpv than DHPAC alone reveals that the effect of DHPAC on PTEN/PI3K/Akt/NF-κB signaling was reversed after phosphatase activity of PTEN being suppressed. These indicated that DHPAC might inhibit PTEN/PI3K/Akt/NF-κB signaling by increasing the activation of PTEN, in association with promoting the transformation of p-PTEN to PTEN. Moreover, the expression of p-Akt and NF-κB in co-treatment of Bpv and DHPAC was lower obviously than Bpv treatment alone. This further

verified that DHPAC inhibited the phosphorylation of PTEN as well as downregulation of Akt expression, resulting in a reduction of NF-κB in the nucleus which suppressed the activation of its target gene products e.g. Bcl-2, Bcl-xl and survivin (Lakshma Nayak et al., 2016). These suggest that the inhibitory effects of DHPAC on proliferation in KB/V cells were closely associated with suppression of PTEN/Akt/NF-κB signaling.

In conclusion, DHPAC, a novel compound that binds to the same colchicine binding site of microtubules, possesses highly potent anti-cancer activities in MDR tumors *in vitro* and *in vivo*. It induces G2/M cell arrest and apoptosis in KB/V cells *in vitro* and inhibits growth of KB/V xenografts in nude mice without any significant cytoxicity. In addition to its binding to microtubule, DHPAC may effect on PTEN in KB/V cells and inhibit PTEN/Akt/NF-κB signaling. Therefore, DHPAC may be a promising agent for the treatment of vincristin-resistant human oral epidermoid carcinoma.

Conflict of interest

Authors declare no conflict of interest.

Acknowledgements

This work was funded by the Natural Science Foundation of China (81373450) and (81573275), the Major Project of Science and Technology of Shandong Province (2015ZDJS04001, 2015ZDXX0301A03) and Collaboration project of Shandong University and South Australia University (2014GJ03).

References

Abdallah, H.M., Al-Abd, A.M., El-Dine, R.S., El-Halawany, A.M., 2015. P-glycoprotein inhibitors of natural origin as potential tumor chemo-sensitizers: A review. J Adv Res 6,

45-62.

Amornphimoltham, P., Sriuranpong, V., Patel, V., Benavides, F., Conti, C.J., Sauk, J., Sausville, E.A., Molinolo, A.A., Gutkind, J.S., 2004. Persistent activation of the Akt pathway in head and neck squamous cell carcinoma: a potential target for UCN-01, Clin Cancer Res. 10,4029-4037.

Binkhathlan, Z., Lavasanifar, A., 2013. P-glycoprotein Inhibition as a Therapeutic Approach for Overcoming Multidrug Resistance in Cancer: Current Status and Future Perspectives. Current Cancer Drug Targets. 13,326-346.

Bulavin, D.V., Higashimoto, Y., Demidenko, Z.N., Meek, S., Graves, P., Phillips, C., Zhao, H., Moody, S.A., Appella, E., Piwnica-Worms, H., Fornace, A.J., Jr., 2003. Dual phosphorylation controls Cdc25 phosphatases and mitotic entry. Nat Cell Biol. 5, 545-551.

Chalhoub, N., Baker, S.J., 2009. PTEN and the PI3-kinase pathway in cancer. Annu Rev Pathol. 4, 127-150.

Chang, L.C., Yu, Y.L., Liu, C.Y., Cheng, Y.Y., Chou, R.H., Hsieh, M.T., Lin, H.Y., Hung, H.Y., Huang, L.J., Wu, Y.C., Kuo, S.C., 2015. The newly synthesized 2-arylnaphthyridin-4-one, CSC-3436, induces apoptosis of non-small cell lung cancer cells by inhibiting tubulin dynamics and activating CDK1. Cancer Chemother Pharmacol. 75, 1303-1315.

Deibler, R.W., Kirschner, M.W., 2010. Quantitative reconstitution of mitotic CDK1 activation in somatic cell extracts. Mol Cell. 37, 753-767.

Fragoso, R., Barata, J.T., 2014. PTEN and leukemia stem cells. Adv Biol Regul56,22-29.

Hafsi, S., Pezzino, F.M., Candido, S., Ligresti, G., Spandidos, D.A., Soua, Z., McCubrey, J.A., Travali, S., Libra, M., 2012. Gene alterations in the PI3K/PTEN/AKT pathway as a mechanism of drug-resistance (review). Int J Oncol. 40, 639-644.

Hwang, D.J., Wang, J., Li, W., Miller, D.D., 2015. Structural Optimization of Indole Derivatives Acting at Colchicine Binding Site as Potential Anticancer Agents. ACS Med Chem Lett . 6, 993-997.

Jordan, M.A., Wilson, L., 2004. Microtubules as a target for anticancer drugs, Nat. Rev. Cancer. 4, 253-265.

Kohnoh, T., Hashimoto, N., Ando, A., Sakamoto, K., Miyazaki, S., Aoyama, D., Kusunose, M., Kimura, M., Omote, N., Imaizumi, K., Kawabe, T., Hasegawa, Y., 2016. Hypoxia-induced modulation of PTEN activity and EMT phenotypes in lung cancers. Cancer Cell Int 16, 1-10.

Lakshma Nayak, V., Nagaseshadri, B., Vishnuvardhan, M.V., Kamal, A., 2016. Investigation of the apoptotic pathway induced by benzimidazole-oxindole conjugates against human breast cancer cells MCF-7. Bioorg Med Chem Lett. 26, 3313-3317.

Lipinski, C.A., Lombardo, F., Dominy, B.W., Feeney, P.J., 2001. Experimental and computational approaches to estimate solubility and permeability in drug discovery and development settings.Adv. Drug Delivery Rev. 41,3–26.

Liu, Y.N., Wang, J.J., Ji, Y.T., Zhao, G.D., Tang, L.Q., Zhang, C.M., Guo, X.L., Liu, Z.P., 2016. Design, Synthesis, and Biological Evaluation of 1-Methyl-1,4-dihydroindeno[1,2-c] pyrazole Analogues as Potential Anticancer Agents Targeting Tubulin Colchicine Binding Site. J Med Chem. 59, 5341-5355.

Loffler, H., Rebacz, B., Ho, A.D., Lukas, J., Bartek, J., Kramer, A., 2006. Chk1-dependent regulation of Cdc25B functions to coordinate mitotic events. Cell Cycle. 5, 2543-2547.

Lu, Y., Chen, J., Xiao, M., Li, W., Miller, D.D., 2012. An overview of tubulin inhibitors that interact with the colchicine binding site. Pharm Res. 29, 2943-2971.

Lu, Y.Y., Wang, J.J., Zhang, X.K., Li, W.B., Guo, X.L., 2015. 1118-20, an indazole diarylurea compound, inhibits hepatocellular carcinoma HepG2 proliferation and tumour angiogenesis involving Wnt/beta-catenin pathway and receptor tyrosine kinases. J Pharm Pharmacol. 67, 1393-1405.

Luqmani, Y.A., 2005. Mechanisms of drug resistance in cancer chemotherapy. Med Princ Pract. 14,35-48.

Molinolo, A.A., Amornphimoltham, P., Squarize, C.H., Castilho, R.M., Patel, V., Gutkind, J.S., 2009. Dysregulated molecular networks in head and neck carcinogenesis. Oral Oncol. 45, 324-334.

Otera, H., Mihara, K., 2012. Mitochondrial dynamics: functional link with apoptosis, Int J Cell Biol. 2012,1-10.

Parker, A.L., Kavallaris, M., McCarroll, J.A., 2014. Microtubules and their role in cellular stress in cancer. Front Oncol. 4, 153.

Patel, N.H., Rothenberg, M.L., 1994. Multidrug resistance in cancer chemotherapy Invest. New Drugs. 12,1-13.

Perez, E.A., 2009. Microtubule inhibitors: Differentiating tubulin-inhibiting agents based on mechanisms of action, clinical activity, and resistance. Mol Cancer Ther 8, 2086-2095.

Schmid, A.C., Byrne, R.D., Vilar, R., Woscholski, R., 2004. Bisperoxovanadium compounds

are potent PTEN inhibitors. FEBS Lett. 566, 35-38.

Schwartz, G.K., Shah, M.A., 2005. Targeting the cell cycle: a new approach to cancer therapy. J Clin Oncol. 23, 9408-9421.

Spinelli, L., Lindsay, Y.E., Leslie, N.R., 2015. PTEN inhibitors: an evaluation of current compounds. Adv Biol Regul. 57, 102-111.

Squarize, C.H., Castilho, R.M., Abrahao, A.C., Molinolo, A., Lingen, M.W., Gutkind, J.S., 2013. PTEN Deficiency Contributes to the Development and Progression of Head and Neck Cancer. Neoplasia. 15, 461-471.

Sun, Z.J., Chen, G., Hu, X., Zhang, W., Liu, Y., Zhu, L.X., Zhou, Q., Zhao, Y.F., 2010. Activation of PI3K/Akt/IKK-alpha/NF-kappaB signaling pathway is required for the apoptosis-evasion in human salivary adenoid cystic carcinoma: its inhibition by quercetin. Apoptosis. 15, 850-863.

Sur, S., Agrawal, D.K., 2016. Phosphatases and kinases regulating CDC25 activity in the cell cycle: clinical implications of CDC25 overexpression and potential treatment strategies. Mol Cell Biochem. 416, 33-46.

Vazquez, F., Devreotes, P., 2006. Regulation of PTEN function as a PIP3 gatekeeper through membrane interaction. Cell Cycle. 5, 1523-1527.

Wang, B., Wang, D., Yan, T., Yuan, H., 2016. MiR-138-5p promotes TNF-alpha-induced apoptosis in human intervertebral disc degeneration by targeting SIRT1 through PTEN/PI3K/Akt signaling. Exp Cell Res. 345, 199-205.

Wang, H.Y., Zhang, Y., Zhou, Y., Lu, Y.Y., Wang, W.F., Xin, M., Guo, X.L., 2016. Rosiglitazone elevates sensitization of drug-resistant oral epidermoid carcinoma cells to

vincristine by G2/M-phase arrest, independent of PPAR-gamma pathway. Biomed Pharmacother. 83, 349-361.

Watanabe, S., Sato, K., Okazaki, Y., Tonogi, M., Tanaka, Y., Yamane, G.Y., 2009. Activation of PI3K-AKT pathway in oral epithelial dysplasia and early cancer of tongue, Bull Tokyo Dent Coll. 50, 125-133.

Wu CF, Liu S, Lee YC, Wang R, Sun S, Yin F, Bornmann WG, Yu-Lee LY, Gallick GE, Zhang W, Lin SH, Kuang J., 2014. RSK promotes G2/M transition through activating phosphorylation of Cdc25A and Cdc25B, Oncogene. 33, 2385-94.

Xie, Y., Naizabekov, S., Chen, Z., Tokay, T., 2016. Power of PTEN/AKT: Molecular switch between tumor suppressors and oncogenes. Oncol Lett. 12, 375-378.

Xu, Y., Zhi, F., Xu, G., Tang, X., Lu, S., Wu, J., Hu, Y., 2012. Overcoming multidrug-resistance in vitro and in vivo using the novel P-glycoprotein inhibitor 1416. Biosci Rep. 32, 559-566.

Yan, J., Pang, Y., Sheng, J., Wang, Y., Chen, J., Hu, J., Huang, L., Li, X., 2015. A novel synthetic compound exerts effective anti-tumour activity in vivo via the inhibition of tubulin polymerisation in A549 cells. Biochem Pharmacol. 97, 51-61.

Yang, H.-Y., Zhao, L., Yang, Z., Zhao, Q., Qiang, L., Ha, J., Li, Z.-Y., You, Q.-D., Guo, Q.-L., 2012. Oroxylin a reverses multi-drug resistance of human hepatoma BEL7402/5-FU cells via downregulation of P-glycoprotein expression by inhibiting NF-κB signaling pathway. Molecular Carcinogenesis. 51, 185-195.

Yue, B., Zhao, C.R., Xu, H.M., Li, Y.Y., Cheng, Y.N., Ke, H.N., Yuan, Y., Wang, R.Q., Shi, Y.Q., Lou, H.X., Qu, X.J., 2013. Riccardin D-26, a synthesized macrocyclic bisbibenzyl

compound, inhibits human oral squamous carcinoma cells KB and KB/VCR: In vitro and in vivo studies. Biochimica et biophysica acta. 1830, 2194-2203.

Zhao, H., Quan, H., Xie, C., Xu, Y., Xie, F., Hu, Y., Lou, L., 2012. YHHU0895, a novel synthetic small-molecule microtubule-destabilizing agent, effectively overcomes P-glycoprotein-mediated tumor multidrug resistance. Cancer Letters. 314, 54-62.

Zhao, X., Tao, X., Xu, L., Yin, L., Qi, Y., Xu, Y., Han, X., Peng, J., 2016. Dioscin Induces Apoptosis in Human Cervical Carcinoma HeLa and SiHa Cells through ROS-Mediated DNA Damage and the Mitochondrial Signaling Pathway. Molecules. 21,1-12.

Figure legends

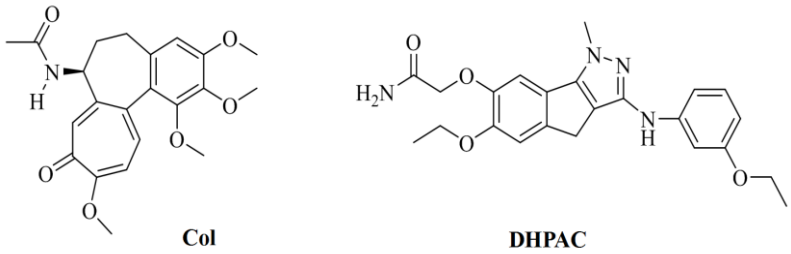

Figure 1. The chemical structure of colchicine and DHPAC

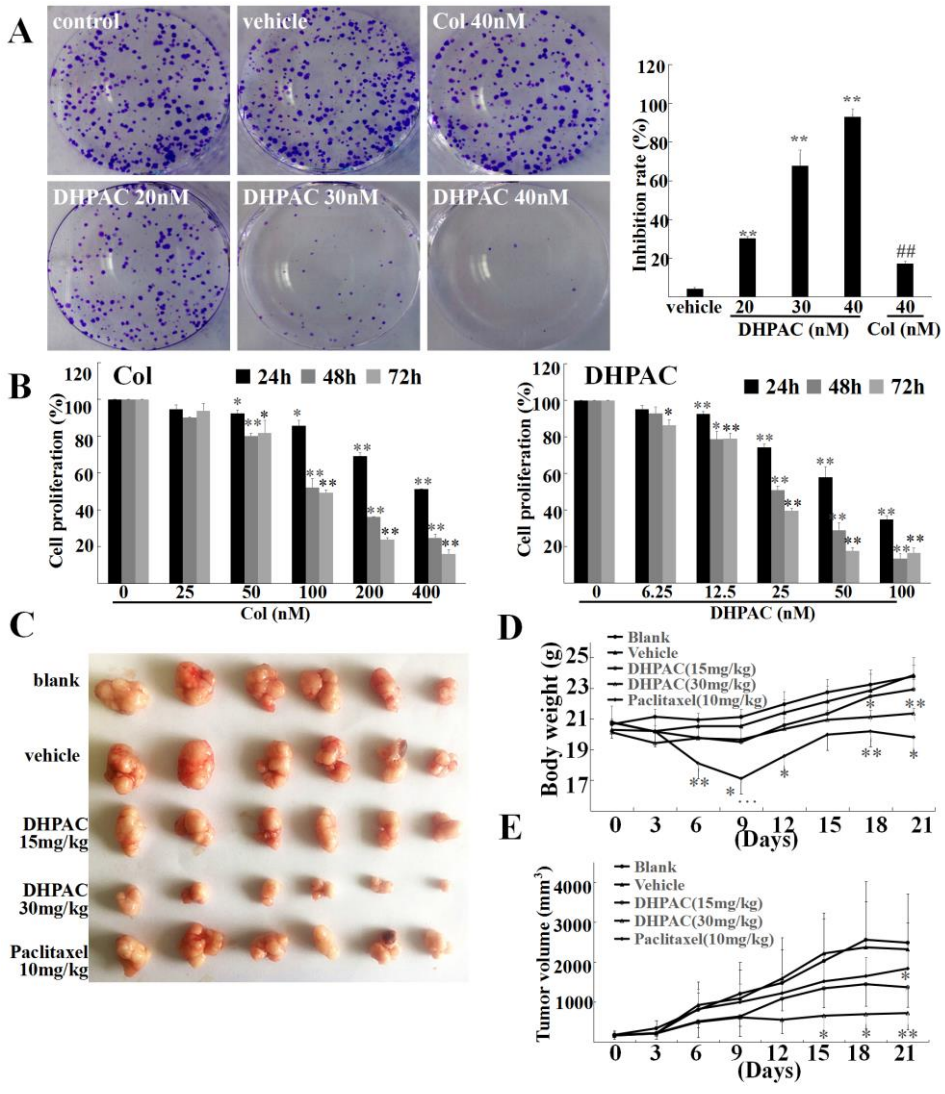

Figure 2. DHPAC inhibits the proliferation of KB/V cells. A. Representative colony formation images of KB/V cells after treatment with DHPAC for 24h, then in DHPAC-free

medium for 12 days. The colonies which were greater than 50 cells were counted under the dissecting microscope and inhibition was denoted as percentage to the control group. B. Cell proliferation was asessed by MTT assay after incubation with DHPAC or colchicine for different time (24h, 48h, 72h). KB/V xenografts were established by inoculating KB/V cells subcutaneously. DHPAC was administrated by intraperitoneal injection every day for 20 days. At the end of experiment, the mice were sacrificed and the tumors were weighed. C, tumor images for each group. The body weight (D) and tumor volume (E) were measured every 3 days. Data are presented as mean ± SD. $^{*}p < 0.05$, $^{**}p < 0.01$ vs. vehicle group; $^{\#\#}p < 0.01$ vs. 40 nM DHPAC group.

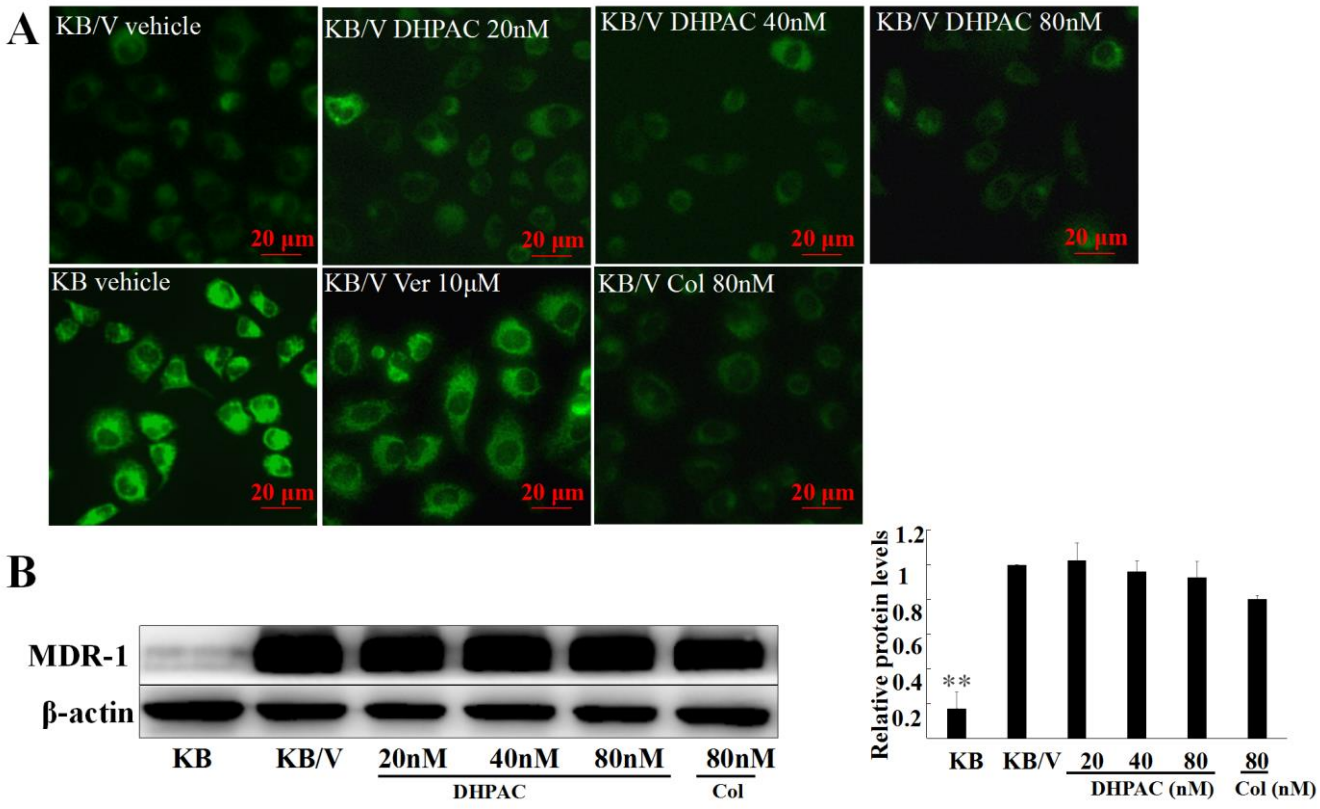

Figure 3. DHPAC has no effect on expression and activity of P-gp in KB/V cells. A. Effect of DHPAC on P-gp activity was evaluated by detecting the intracellular accumulation of Rh123. KB/V cells were treated with vehicle medium (0.4% DMSO medium), verapamil, colchicine

and different concentrations of DHPAC, and KB cells were treated with vehicle medium, then stained with Rhodamine 123, and photographed under fluorescence microscopy (20× magnification; scale bar = 20μm). B. The expression of P-gp in KB/V cells was detected and quantized using Western blotting. Triplicate experiments were performed. $^{**}P < 0.01$ vs. KB/V vehicle group.

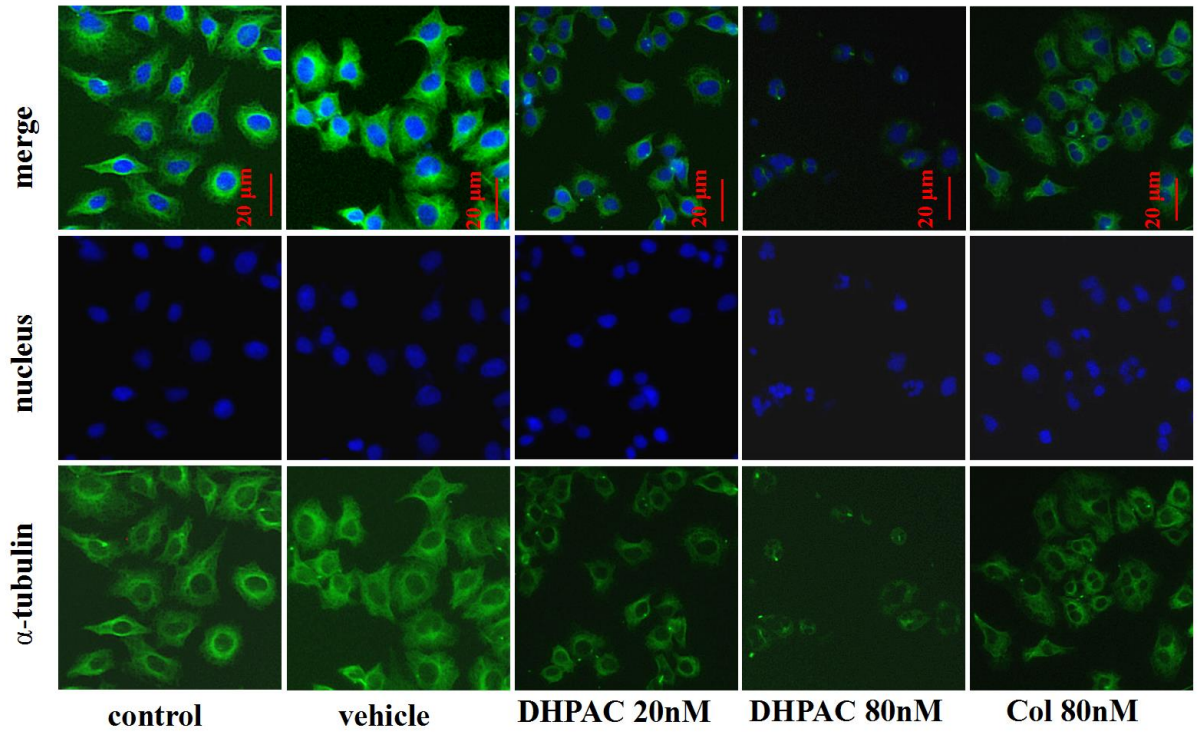

Figure 4. DHPAC inhibits cellular microtubule network in KB/V cells . Cells were treated with blank (10% FBS medium), control (0.4% DMSO), DHPAC (20 nM, 80 nM) or colchicine (80 nM) for 24h before images of the cells were taken by fluorescence microscopy (20× magnification; scale bar = 20μm). Microtubules were labeled by anti-α-tubulin antibody with FITC-conjugated secondary antibody (green), and nucleus was labeled with hoechst 33342 (blue).

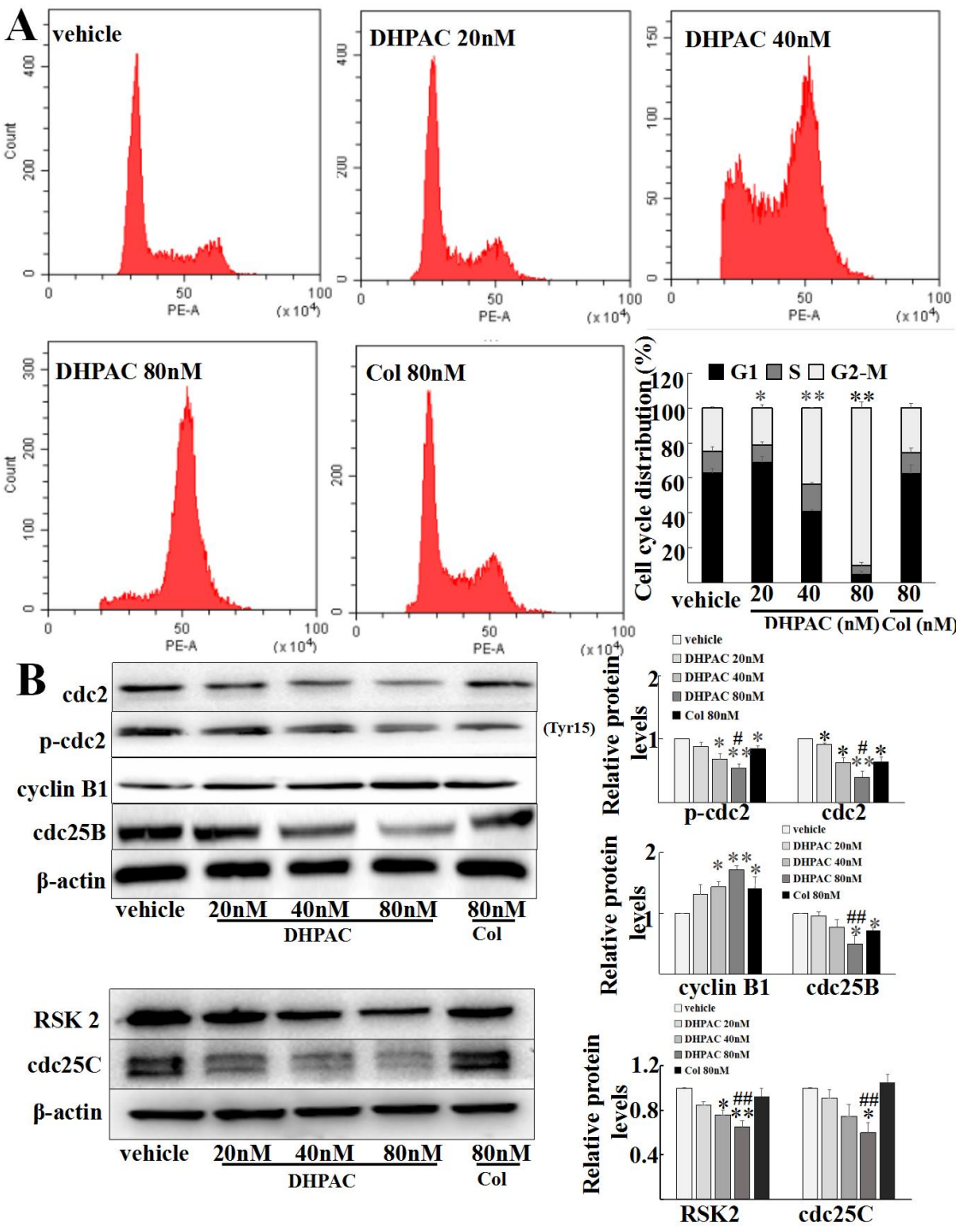

Figure 5. DHPAC arrests KB/V cells in G2/M phase by regulating the expression of G2/M related proteins. A. Cells were treated with different concentrations of DHPAC or colchicine (80nM) for 24 h and followed by cell cycle analysis by flow cytometry. B. The expression of G2/M regulatory proteins was detected by Western blotting (mean ± SD, n=3). $^{*}P < 0.05$, $^{**}P < 0.01$ vs. control group. $^{\#}P < 0.05$, $^{\#\#}P < 0.01$ vs. colchicine group.

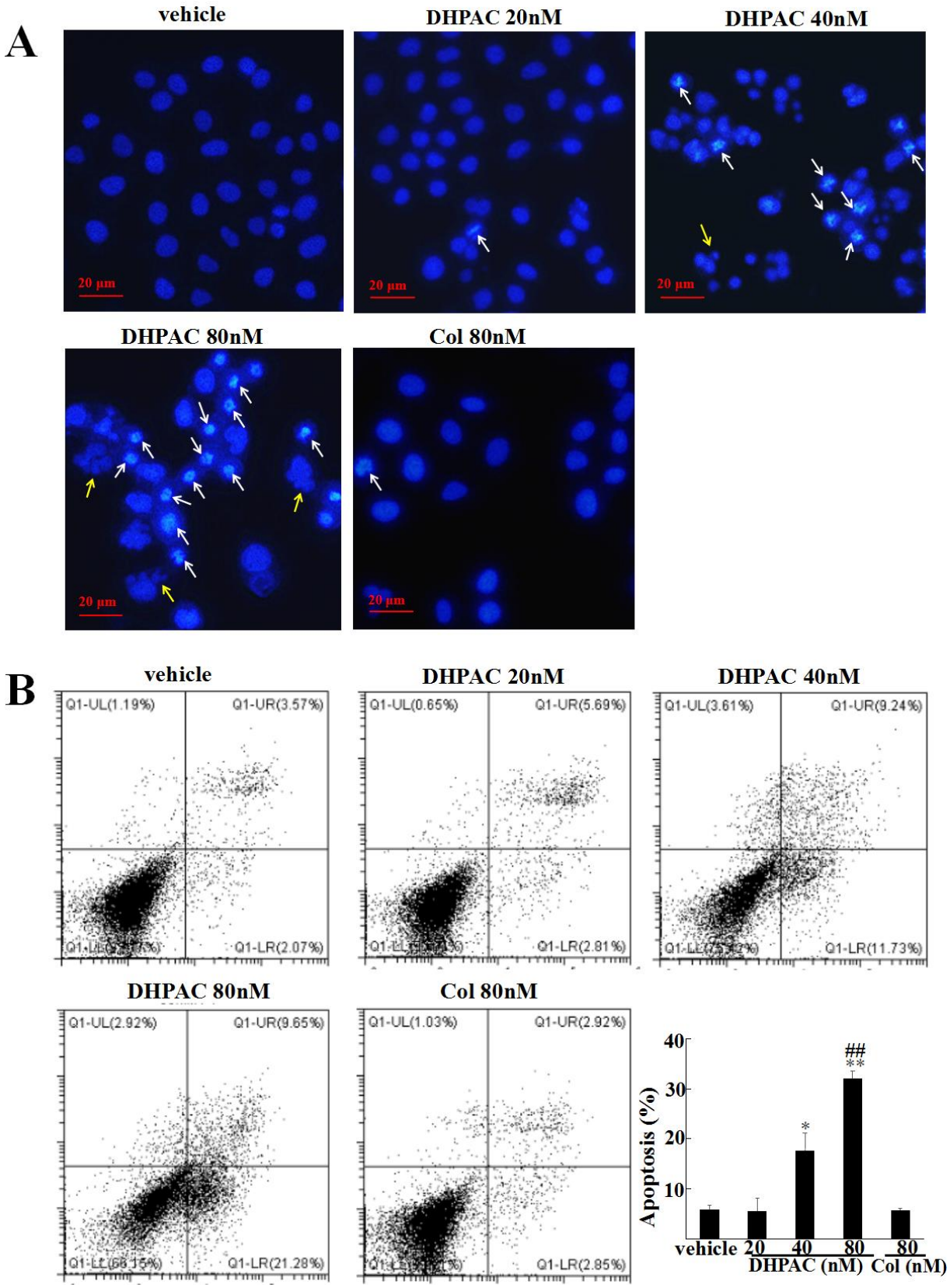

Figure 6. DHPAC induces apoptosis in KB/V cells. A. Cells were treated with different concentrations of DHPAC or colchicine (80 nM) for 24 h, before stained with hoechst 33342.

White arrows indicated characteristics of chromatin condensation, yellow arrows indicated apoptotic bodies. B. Apoptotic cells was detected by Annexin-FITC and PI double-staining and analyzed by flow cytometry. live cells (Q1-LL), early apoptotic cells (Q1-LR), late apoptotic cells (Q1-UR) were indicated (mean ± SD, n=3). $^{*}P < 0.05$, $^{**}P < 0.01$ vs. vehicle group; $^{\#\#}P < 0.01$ vs. colchicine group.

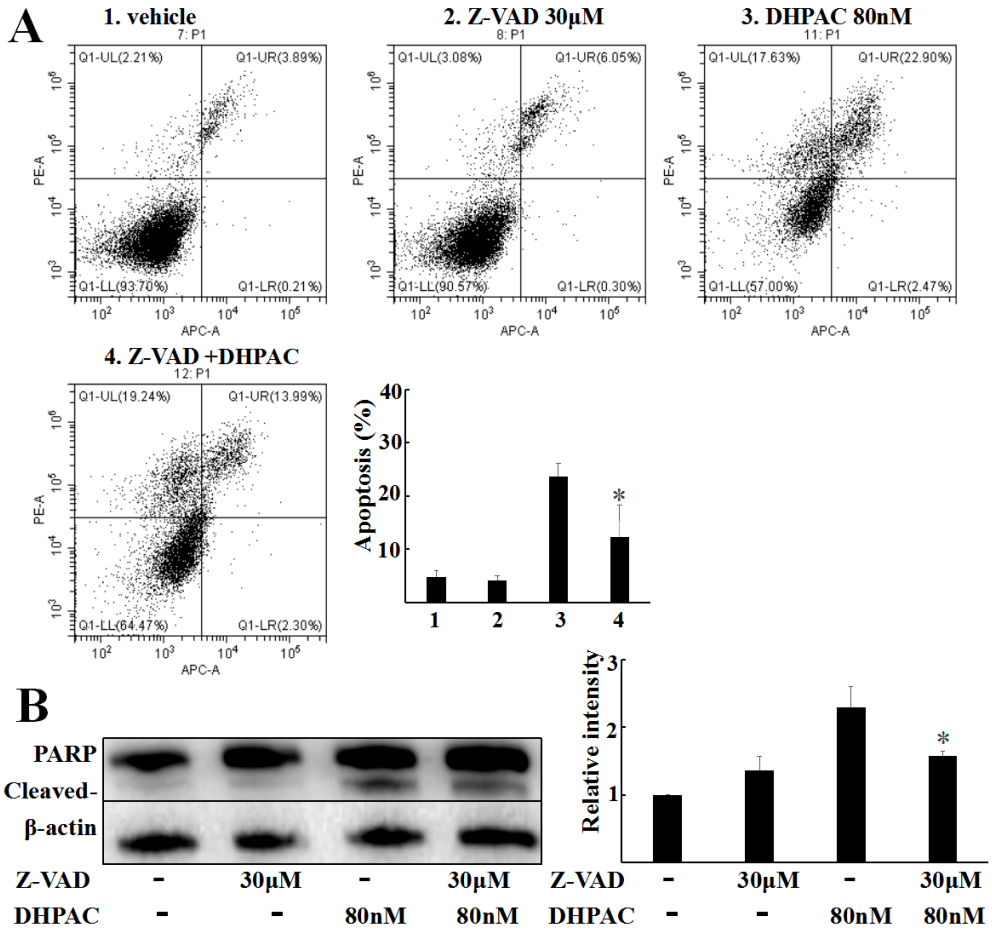

Figure 7. DHPAC induced-apoptosis was inhibited by z-VAD. A. KB/V cells were pretreated with Z-VAD-FMK (30 μM) for 1 h before exposure to 80nM DHPAC for 48h. Apoptotic cells were detected by Annexin-FITC and PI double-staining and analyzed by flow cytometry. B. Apoptotic-related protein PARP was detected by Western blotting (mean ± SD, n=3). $^{*}P < 0.05$ vs. 80 nM DHPAC group.

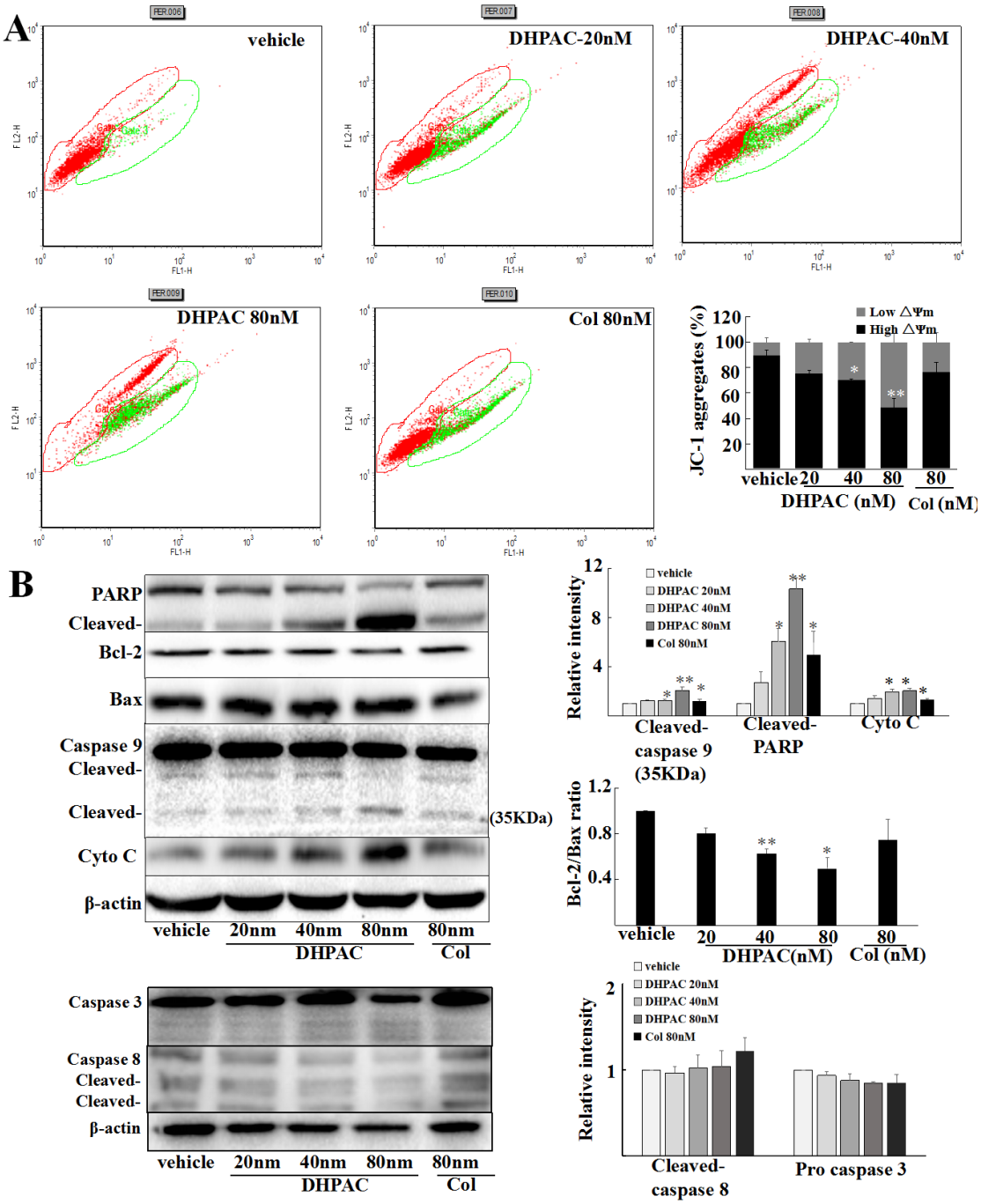

Figure 8. DHPAC induces apoptosis of KB/V cells. A. after exposure to different concentrations of DHPAC or colchicine (80nM) for 48 h, KB/V cells were stained by JC-1 and analyzed by flow cytometry for mitochondrial depolarization. The red and green gates represent high and low mitochondrial potential, respectively. B. Apoptosis-related proteins were detected by Western blotting (mean ± SD, n=3). $^{*}P < 0.05$ and $^{**}P < 0.01$ vs. control. $^{\#}P$

< 0.05 vs. colchicine group.

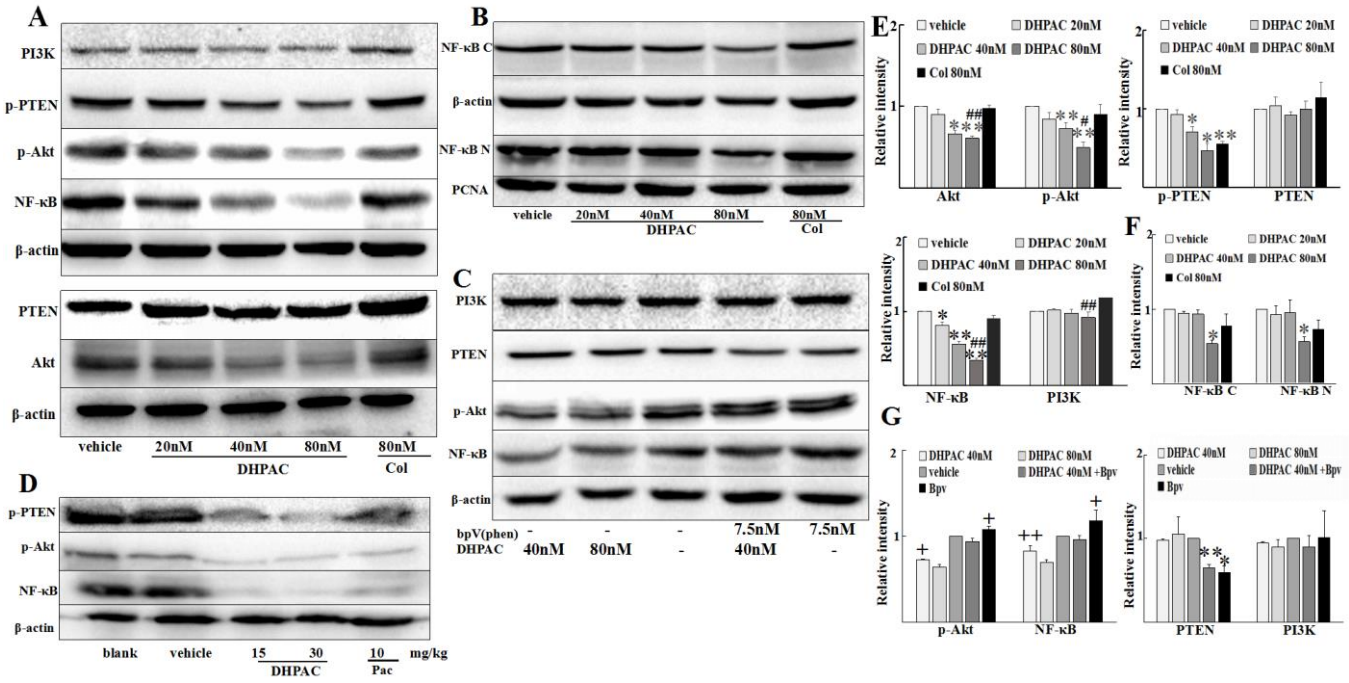

Figure 9. DHPAC inhibit KB/V cell growth by suppressing PTEN-Akt-NF-κB signaling. A. KB/V cells were incubated with DHPAC (20nM, 40nM, 80nM) and colchicine 80 nM for 24h followed by analysis of the expression of PI3K, Akt, PTEN, p-Akt, p-PTEN (Ser380/Thr382/Thr383), and NF-κB in KB/V cells by Western blotting. B. NF-κB was detected both in cytoplasm (NF-κB C) and nucleus (NF-κB N) after treatment with DHPAC or colchicine. C. Representative blots of PI3K, PTEN, p-Akt and NF-κB in KB/V cells treated with DHPAC for 24h with or without PTEN inhibitor bpV (phen) are shown. D. Representative blots of PTEN/Akt/NF-κB signaling proteins in KB/V cells xenografts are shown. E, F, G: Quantification and statistical analysis of the protein bands in A, B and C, respectively. Data are expressed as mean ± SD (n=3). $^{*}P < 0.05$, $^{**}P < 0.01$ vs. vehicle group. $^{+}P < 0.05$, $^{++}P < 0.01$ vs. 40 nm DHPAC co-treated with Bpv group.

Table 1. Resistance determination of different drug resistant cell lines at 48h (mean ± SD, n=3)

Drugs	IC_{50}		RF
	KB	KB/V	
vincristine	3.7 ± 0.1nM	427.3 ± 28.3nM	115
paclitaxel	20.0 ± 3.1nM	574.9 ± 20.9nM	29
	BEL7402	Bel7402/5-FU	
5-fluorouracil	0.2 ± 0.06mM	31.2 ± 9.2mM	164
	MCF-7	MCF-7/A	
doxorubicin	2.6 ± 0.8μM	22.7 ± 8.1μM	8

RF (resistant fold) = IC_{50} against resistant cells/ IC_{50} against sensitive cells.

Table 2. IC_{50} values of DHPAC and colchicine against various human cancer cell lines for 24h (mean ± SD, n=3)

	IC_{50} (nM)	
Cell lines	DHPAC	colchicine
Bel7402	88.3 ± 11.9	91.7 ± 27.0
Bel7402/5-FU	226.3 ± 34.4	296.7 ± 64.9
KB	47.4 ± 1.6	34.2 ± 1.6
KB/V	64.4 ± 2.8	458.0 ± 34.1
MCF-7	60.0 ± 4.9	77.0 ± 14.6
MCF-7/A	281.3 ± 30.8	334.0 ± 29.5

Table 3. IC_{50} values of DHPAC and colchicine against KB/V and KB cells at different times points (mean ± SD, n=3)

Drugs	IC_{50} (nM)		
	24h (KB/V / KB)	48h (KB/V / KB)	72h (KB/V / KB)
DHPAC	64.4 ± 2.8 / 46.3 ± 1.4	29.3 ± 2.5 / 28.7 ± 3.7	23.8 ± 1.8 / 23.5 ± 3.2
colchicine	458.0 ± 34.1 / 33.1 ± 1.6	138.2 ± 1.2 / 14.6 ± 0.7	120.0 ± 9.1 / 7.6 ± 0.7

Table 4. Inhibitory effects of DHPAC on growth of KB/V xenografts in athymic mice (mean ± SD)

Groups	Mice (n) initial/en	Body weight (g) initial/end	Tumor weight (g)	Inhibition rate (%)
Blank	6/6	20.6 ± 0.4 / 23.8 ± 0.7	2.2 ± 1.0	—
Vehicle	6/6	20.3 ± 0.4 / 23.8 ± 1.1	2.1 ± 0.8	—
DHPAC 15 mg/kg	6/6	20.8 ± 1.0 / 22.9 ± 0.7	1.5 ± 0.3*	25.1
DHPAC 30 mg/kg	6/6	20.1 ± 0.8 / 21.4 ± 0.4	0.5 ± 0.2**	75.8
Paclitaxel 10 mg/kg	6/6	20.7 ± 0.4 / 19.8 ± 1.8*	1.7 ± 0.5	24.1

*P < 0.05, **P < 0.01 vs. vehicle group.

Note: The data of body weight (end) for statistical analysis have been deducted tumor weight.